Control of flow on helicopter rotor blades under quasi-steady and unsteady conditions using smart air-jet vortex generators

Chrisminder Singh*, David J Peake*, Anastasios Kokkalis*,
Frank Coton+ and Roderick Galbraith+

***Centre for Aeronautics, City University, London UK**
+ Department of Aerospace Engineering, University of Glasgow, UK

Abstract

Low-speed wind tunnel experimental investigations were conducted to explore the use of smart air-jet vortex generators (AJVGs) to delay flow separation over a rotor blade section under quasi-steady and unsteady flow conditions. Utilising only a small amount of continuous blowing ($0.0\%<C_\mu<1.0\%$), we have been successful in suppressing the formation of the dynamic stall vortex (and the corresponding break in the pitching moment curve) of an oscillating RAE 9645 aerofoil. We have also found that we can reduce the mass flux (and ensuing momentum) requirement of AJVGs by means of pulsing whilst simultaneously maintaining performance enhancements attributable to steady AJVGs on a quasi-steady NACA 23012C aerofoil.

Nomenclature

AJVG	air-jet vortex generator
b	aerofoil span
c	aerofoil chord
C_{DP}	wake profile drag coefficient
C_N	normal force coefficient
$C_{M(0.25c)}$	quarter-chord pitching moment coefficient
C_P	static pressure coefficient
C_μ	Blowing momentum coefficient $= (\dot{m}\, V_J) / (0.5\, \rho\, U^2_\infty\, c)$
f	dominant pulsing frequency
F+	dimensionless pulsing frequency ($f\, L/U_\infty$)
k	reduced frequency, ($\omega\, c/2U_\infty$)
L	distance from actuator to aerofoil trailing edge
$\dot{m}$	AJVG mass flow rate
M	Mach number
R_{ec}	Reynolds number based on aerofoil chord
t	time
U_∞	freestream axial velocity
V_J	jet velocity at AJVG exit
α	angle of attack
α_m	mean angle of attack
ϕ	angle of pitch of AJVG relative to local surface tangent at aerofoil surface
ψ	angle of skew of AJVG relative to local surface tangent at aerofoil surface
ω	rotational frequency, rad/s
ρ_∞	freestream fluid density

1. Introduction

Dynamic stall is encountered when an aerofoil experiences a dynamic change of angle-of attack. It is characterised by the formation, migration and shedding of a leading-edge vortex or dynamic stall vortex. The movement of this vortex as it migrates and sheds from the aerofoil trailing edge contributes to large lift and moment overshoots in excess of static values, and leads to significant non-linear hysteresis in the aerofoil force and moment behaviour.

It is well known that rotor blade dynamic stall substantially limits the overall performance of rotorcraft in forward flight. Thus, understanding and suppressing the dynamic stall vortex that is formed under dynamic stall conditions is a major research area of interest in rotorcraft; for the ability to suppress the formation of the dynamic stall vortex will enhance the performance of the helicopter rotor and hence expand the helicopter flight envelope and vehicle utility.

The most common techniques used at present to alleviate dynamic stall include the active control of blade pitch as well as the passive control of blade response through structural tailoring[1]. The latter may be achieved by the optimisation of the blade twist distribution along the blade radius, careful blade planform design as well as through the use of multi-aerofoil sections along the rotor radius – thick, high lift sections inboard and thin, transonic sections for the tip region, whereby the blade disc loading is distributed efficiently.

Alternatively, control of the dynamic stall process may be achieved through the use of low momentum AJVGs. They consist of small air jets emerging from an aerodynamic surface that are pitched and skewed relative to the oncoming freestream flow. The interaction between the air-jets and the freestream flow forms well-organised vortical structures with 'powered' cores that are capable of withstanding especially severe adverse pressure gradients as they penetrate downstream. Previous work, see Ref. 2, conducted at City University demonstrated the successful application of this active control system on a NACA 23012C aerofoil under quasi-steady flow conditions. In those tests, steady AJVGs successfully delayed stall onset by up to 6^0, increased lift by up to 25%, reduced overall drag by up to 50%, and extended the lift/drag envelope accordingly[2].

This paper focuses on research conducted at the University of Glasgow to study the application of steady AJVGs for the control of dynamic stall. Concurrently, research conducted at City University is aimed at exploiting the aerodynamic efficiency of pulsing the AJVGs. The potential benefit of doing so is to further reduce the mass flux and momentum requirements whilst maintaining the aerodynamic performance enhancements achieved by the steady AJVGs.

Success in both areas will enable the utilisation of a low energy system to control the entire rotor viscous flow, from subsonic along the principal lifting section of the blade to transonic at the tip. Careful consideration of the AJVGs' installation is required, however, in order to keep the rotor blade design as uncomplicated and as inexpensive as possible, due to life-cycle frequent blade replacement.

2. Experimental Arrangement

2.1. Steady blowing AJVGs under unsteady flow conditions

Tests were conducted on a vertically mounted RAE 9645 aerofoil in the Handley-Page wind tunnel at the University of Glasgow. This is a closed return type tunnel. The test Reynolds number was $1.5\text{x}10^6$ and the Mach number was 0.13, based on chord and freestream conditions. The aerofoil model had a chord of 0.5 m and an aspect ratio of 2.7. It was constructed using a fibreglass skin filled with epoxy foam and bonded to an aluminium spar. The model was pitched about the quarter-chord point using a linear hydraulic actuator and crank mechanism[3].

The model was instrumented with 30 dynamic pressure transducers, Sensor Technics SCS05GSMT, positioned along the mid-span chordline. Output signals from the transducers were taken to a specially designed signal-conditioning unit with its own control board. On instruction from the computer, the control board automatically removed all offsets to below the A-D converter resolution and adjusted all gains as necessary. A 486-based PC interfaced to propriety Bakker Electronics BE256 A-D modules carried out the data acquisition. Each A-D channel has a maximum sampling rate of 50kHz; such a high rate is required to capture the fine detail of the dynamic stall process, especially at the relatively high oscillatory reduced frequencies tested, i.e. $0.01 < k < 0.2$. Tests for the oscillating aerofoil with a sinusoidal-pitching motion are defined by

$$\alpha = \alpha_m + 10^0 \sin(\omega t)$$

where, in this case,

$$\alpha_m = 15^0 \text{ and } 0.2897 \leq \omega \leq 5.0627$$

The sampled data were averaged over 4 cycles.

2.2. Intermittent blowing AJVGs under quasi-steady flow condition

These tests were conducted in the T2 low-speed wind tunnel at City University on a NACA 23012C aerofoil. The T2 is a closed-circuit type wind tunnel with a working section of 0.81m x 1.12m and a length of 1.68m. The aerofoil model had a chord of 0.48m and a span of 0.74m. It was mounted vertically in the working section between two endplates at model mid-chord. Tangential blowing on the endplates was used for the control of the boundary layer growth at the aerofoil/endplate junction. Thus a nominally two-dimensional flow across the span over the entire incidence range tested was reasonably maintained. The desired angle of attack was set by rotating the model about the spindle axis on two sets of thrust roller bearings. The angle of attack tested was in the range $6^0 < \alpha < 21^0$.

Chordwise measurements of surface pressure were obtained from (a), 84 static pressure tappings evenly distributed at three spanwise locations (0.26b, 0.51b, 0.62b); and (b), 7 dynamic pressure transducers, Kulite CTQH 187, positioned at 0.47b. Wake total pressure profiles were measured at the model centreline one-chord length downstream of the aerofoil. The measurement of the chordwise static pressure distribution and wake properties were made using 3 Scanivalves (Type 48S3) connected to a CED 1401 data acquisition system. The dynamic pressure transducer data were first amplified and signalled conditioned by means of a transducer amplifier (FLYDE 379TA) unit and then logged using a CED1401*plus* data acquisition system.

2.3. Air-jet vortex generators (AJVGs)

The geometrical design and spacing of the AJVGs installed on both the RAE 9645 and NACA 23012C were based on the recommendations outlined by Pearcey[4,5] and Freestone[6]. Both models were configured with two chordwise sets of AJVG arrays, one located at x/c=0.12 and the other at x/c=0.62 (see Figure 1). The RAE 9645 had a total of 28 AJVGs placed along the span at each of the two chordwise positions, whilst the NACA 23012C had 15 AJVGs. The AJVGs were spaced at intervals of 0.1c along the span and had a rectangular geometric shape. The jet slot aspect ratio was approximately 5, with the exit jet pitched at 30^0 and skewed at 60^0 relative to the surface tangent (see Figure 2).

Air is supplied to the AJVG arrays via two pressure regulated plenum chambers located within the aerofoil section. Intermittent blowing was attained via a "puffer" assembly consisting of a rotor disc sandwiched between two stator discs, each with 8 equispaced radial slots. For the tests, the AJVGs were operated at low blowing momentum coefficients, both mean and root-mean-square, of between $0.2\%<C_\mu<1\%$, over a wide range of reduced pulsing frequencies of $0<F^+<2.0$.

3. Results and discussion

The current experimental research is aimed at demonstrating,

a) effectiveness of steady AJVGs to modify the onset of dynamic stall of an oscillating aerofoil and
b) possibility of maintaining the aerodynamic performance enhancements attributable to steady blowing whilst reducing the mass flux and momentum requirements under pulsing conditions.

The examination of results obtained from these experimental tests is conducted in the following sections.

3.1. Quasi-steady and dynamic stall steady blowing tests

3.1.1. Quasi-steady tests

Experiments were initially conducted to study the behaviour of the RAE 9645 aerofoil under quasi-steady flow conditions. The cleanfoil* chordwise pressure distribution variation with incidence, at the centre span location, is depicted in Figure 3. Examination of the test data shows that at $\alpha=10^0$, there is no evidence of flow separation; the flow is fully attached over the entire aerofoil upper surface#. As incidence increases to $\alpha=15^0$, there is evidence of flow separation at the trailing edge region, back to approximately 80% chord. Further increasing the incidence, causes the separated flow region to move slowly upstream, towards the leading edge.

* Cleanfoil is defined as an aerofoil installed with AJVGs C_μ=0.0
# A pressure transducer was not installed at the aerofoil trailing edge due to (a), space constraints and (b), the necessity to avoid data aliasing and biasing [occurs when a pressure transducer is connected to the measuring location with a long tubing].

At α=18^0, it is seen that flow separation covers almost the entire aerofoil upper surface.

The effectiveness of steady AJVGs, under quasi-steady flow conditions, to mitigate separation, increase C_N values, and delay stall is depicted in Figures 4-6. Figure 4 shows that using low momentum blowing, C_μ = 0.01, from the front AJVG array alone (i.e. at x/c=0.12) or from both the front and rear arrays simultaneously, with a combined C_μ = 0.01 (i.e. at x/c=0.12 & x/c=0.62) is effective in delaying separation and maintaining top surface suction at α=18^0. Figure 5 shows that blowing only from the front AJVG array (C_μ=0.01) offers a measurable advantage over blowing from the combined front and rear AJVG arrays ($C_{\mu TOTAL}$=0.01) in its ability to restore and increase peak suction around the leading edge region at α=18^0. Whereas, blowing from the rear array alone (i.e. at x/c=0.62) provides a small suction pressure enhancement around the leading edge region; but fails to fully reattach the highly separated flow at this high incidence angle.

Figure 6 shows the benefits gained by the introduction of steady AJVGs on the normal force coefficient (C_N), stall angle (α_s) and quarter chord pitching moment break angle ($\alpha_{C_{M(0.25c)}}$) of the RAE 9645 aerofoil. The effectiveness of blowing from the front AJVG array is further emphasised by the increase in the C_{Nmax} value – up to 21% - when compared to that attained when blowing from either the front and rear, or the rear AJVG array only (i.e. up to 14% and 7% respectively). Furthermore, blowing from the front AJVG array delayed the stall angle and moment break angle by up to 5^0 and 8.5^0, i.e. α_s=19.0^0 and $\alpha_{C_{M(0.25c)}}$ =22.5^0 respectively. Blowing from the front and rear AJVG arrays simultaneously, delayed the appearance of stall by 4.5^0 (i.e. up to α_s=18.5^0). It also shows that, in this case, the aerofoil experiences a sudden and drastic loss in C_N, after α_s, as opposed to the gradual decrease in C_N observed when utilising blowing from the front AJVG array only. Similar observations can be noted in the quarter-chord pitching moment curves, where the moment break angle is delayed by about 4.5^0 only, i.e. $\alpha_{C_{M(0.25c)}}$ =18.5^0. The inability of the combined front and rear array blowing, at a combined total C_μ of 0.01, to negotiate the adverse pressure gradient associated with high incidence angles significantly limits its ability to sustain performance enhancements for the higher range of angle of attack.

3.1.2. Dynamic Stall tests

Having established the effectiveness of steady AJVGs on the RAE 9645 aerofoil under quasi-steady flow conditions, further experiments were conducted to determine the potential of steady AJVGs to control dynamic stall. Figures 7-9 show that front array steady AJVGs successfully (and beneficially) modify the onset as well as reduce the severity of dynamic stall on a sinusoidally oscillating RAE 9645 aerofoil.

In particular, Figures 7 (a) and (b) depict the development of C_N and $C_{M(0.25c)}$ versus angle of attack for both the cleanfoil and front AJVG array blowing cases at two reduced oscillation frequencies, k=0.052 and 0.103. Data analysis for the cleanfoil shows that at the higher reduced oscillation frequency, k=0.103, there is a significant non-linear increase in the lift-curve slope followed by the sudden and severe lift and moment breaks. Whereas, for the lower reduced oscillating frequency case, k=0.052, the magnitude of these effects is less. This indicates that the dynamic stall vortex formed increases in strength with increasing reduced oscillation frequency. The migration and shedding of this vortex causes the non-linear lift-curve slop increase and breaks in the lift and pitching moment curve respectively. The second increase in lift-curve slope seen after the primary vortex has shed from the aerofoil, i.e. after the first large and sudden decrease in C_N, indicates the formation of a secondary vortex at the leading edge. However the additional lift and moment increase and break is less in value and severity suggesting that this secondary vortex is much weaker.

Instantaneous chordwise pressure distributions, depicted in Figure 8(a) and 9(a), show that with increasing angle of attack, the aerofoil peak suction increases, up to P1, due to the existence of very strong vortical flow in the leading edge region[7,8]. Further increase leads to a collapse in this peak suction due to the vortex migration downstream towards the trailing edge.

The pressure distributions of Figures 8(a) and 9(a) also show the presence of a secondary suction peak, P2, which can be associated with development of vortical flow at the leading edge region. This secondary dynamic stall vortex is not only weaker but also smaller compared to the primary stall vortex[7,8]. Additionally, the instantaneous pressure distributions also confirm the previously made observation that a stronger vortex forms, mitigates and sheds when the aerofoil is oscillating at k=0.103 (see Figures 8(a) and 9(a)).

The introduction of steady blowing from the front array of AJVGs is aimed at controlling or eliminating the dynamic stall vortex. Figures 7-9 show that the front AJVG blowing successfully weakens and delays the shedding of the primary whilst completely eliminates the secondary dynamic stall vortex. As a result of this, it acts to delay lift and pitching moment stall whilst simultaneously it reduces the magnitude of the lift and pitching moment break (see Figures 7(a) and (b)).

Instantaneous chordwise pressure distributions with blowing from the front array AJVG shows the recovery and increase of the leading edge peak suction and the non-existence of the secondary dynamic stall vortex (see Figures 8(b) and 9(b)). Furthermore, the front array AJVG reduces the magnitude of the hysterisis loop in both the C_N and $C_{M(0.25c)}$ vs. angle of attack plots. It is hypothesized that this is achieved by promoting the reattachment of the separated boundary layer on the downstroke motion of the aerofoil[9].

3.2. Quasi-steady pulsed blowing tests

Seifert et al [10,11] and McManus et al [12, 13], have successfully studied the effectiveness of using intermittent blowing as a flow control mechanism. The potential benefit of incorporating this idea to suppress dynamic stall has led to the initiation of preliminary pulsed AJVGs experimental investigations at City University.

The blowing momentum coefficient in this case is given in the form of [$C_\mu \approx$(steady level, unsteady level)%]. The Duty Cycle (DC) of the pressure signal is defined as the ratio of the jet open time to the pulse period. In the experiments conducted, the DC was approximately 0.65. An example of the pressure pulse signal measured inside the plenum chamber for a supplied pressure level of 0.1psi(g) mean and 0.078psi(g) unsteady at F^+=0.7, is shown in Figure 10.

Figures 11-13 show experimental results employing steady and pulsed blowing from the front array of AJVGs on the NACA 23012C aerofoil to control the grossly stalled flow at α=20^0. The reattachment of the stalled flow with steady blowing from the front array AJVGs at [$C_\mu \approx$(0.40, 0.0)%; F^+=0.0] is clearly shown by the chordwise pressure coefficient distribution plot of Figure 11. It is observed that steady blowing enhances both the upper and lower surface pressure coefficient distribution. The benefit of flow control due to the active AJVGs is further emphasised by the considerable improvement in the leading-edge pressure suction peak and the reduction in the wake momentum deficit, as shown in Figures 12 and 13 respectively.

Reducing the steady state $C\mu$ to 0.27%, i.e. [$C_\mu \approx$(0.27, 0.0)%; F^+=0.0], significantly diminishes any flow control benefits. As a result, the region of separated flow over the aerofoil moves forward from the trailing edge to approx. 30%-chord, refer to Figure 11. The reduction in flow control effectiveness is further emphasised by the considerable increase of the magnitude and width of the wake momentum deficit, as shown in Figure 13. Pulsing the AJVGs at the steady and unsteady levels of either [$C_\mu \approx$(0.26, 0.09)%; F^+=0.7] or [$C_\mu \approx$(0.26, 0.05)%; F^+=1.3] leads to the re-establishment of the aerofoil performance to an equivalent status of control achieved at the higher steady level blowing of [$C_\mu \approx$(0.40, 0.0)%; F^+=0.0], see Figures 11, 12 & 13.

Overall, these preliminary tests show that the effect of pulsing in saving mass flux (and consequently momentum) whilst maintaining overall performance is definite. Further detailed research and development is needed, however, in order to optimise the system. Test plans to optimise the system are presently been formulated.

4. Conclusions

It has been demonstrated that the utilisation of AJVGs in the RAE 9645 and NACA 23012C aerofoils, leads to the considerable enhancement of the aerodynamic performance characteristics.

These include (a), the amelioration of dynamic stall with relatively low-blowing momentum coefficients; and (b), a reduction of the blowing mass flux and momentum required to suppress separation by pulsing the AJVGs. The applications of either steady or pulsed AJVGs as a means of viscous flow control on the helicopter rotor may hence be of particular interest to the rotorcraft industry. The potential to:

- enhance the performance characteristics around the high-lift producing radial blade locations,
- reduce shock induced boundary-layer separation at the tip[4], and,
- assuage dynamic stall

should permit a step function improvement in overall rotor-blade performance

Acknowledgements

The work was carried out with funding from the Engineering & Physical Science Research Council, (Grant Ref GR/M85432/01), Westland Helicopters and DSTL (formerly DERA). The authors acknowledge with gratitude the help and support of their sponsors and, in particular, the substantial contributions of Mr C. Barber, Mr M. Smith and Mr R. Gilmour to this work.

References

1. Khanh Nguyen, “Active Control of Helicopter Blade Stall”, Journal of Aircraft, January 1998, Vol 25,(1), pp91-98

2. Lewington, N.P., Peake, D.J., Henry, F.S., Kokkalis, A. and Perry, J., “The Control the Flow on Helicopter Rotor Blades”, Proc. of 26th European Rotorcraft Forum, 26-29 September 2000, The Hague, Netherlands

3. Coton, F.N., and Galbraith, R.A.McD., “An experimental study of dynamic stall on a finite wing”, The Aero Journal, May 1999, No 2429, pp229-236

4. Pearcey, H.H., “Shock induced separation and its prevention by design and boundary layer control”, Pergamon Press, pp1166-1134, 1961

5. Pearcey, H.H., Rao, K., and Sykes, D.M., “Inclined air-jets used as vortex generators to suppress shock induced boundary layer separation”, AGARD-CP-534, Paper 40, 1993

6. Freestone, M.M., “Preliminary tests at low speed on vorticity produced by air-jet vortex generators”, RM 85/1, Centre for Aeronautics, City University, 1985

7. Carr, L.W., “Progress in Analysis and Prediction of Dynamic Stall”, Journal of Aircraft, January 1988, Vol 25, (1), pp 6-17

8. McCroskey, W.J., “The Phenomenon of Dynamic Stall”, NASA Technical Memorandum 81264, 1981

9. Weaver, D., McAlister, K.W., and Tso, J., “Suppression of Dynamic Stall by Steady and Pulsed Upper-Surface Blowing”, 16th AIAA Applied Aerodynamics Conference, June 15-18, AIAA 98-2413

10. Seifert, A., Bachar, T., and Wygnanski, I., “Oscillatory blowing, A Tool to Delay Boundary Layer Separation”, 31st Aerospace Sciences Meeting & Exhibit, January 11-14, 1993, AIAA 93-0440

11. Seifert, A., Daraby, A., Nishri, B., and Wygnanski, I., “The Effects of Forced Oscillations on the Performance of Airfoils”, AIAA Shear Flow Conference, July 6-9, 1993, AIAA 93-3264

12. McManus, K.R., Legner, H.H., and Davis, S.J., “Pulsed Vortex Generator Jets for Active Control of Flow Separation”, 25th AIAA Fluid Dynamics Conference, June 1994, AIAA 94-2218

13. McManus, K., and Magill, J., “Airfoil Performance Enhancement Using Pulsed Jet Separation Control”, 28th AIAA Fluid Dynamics Conference, June 29-July2, 1997, AIAA 97-1971

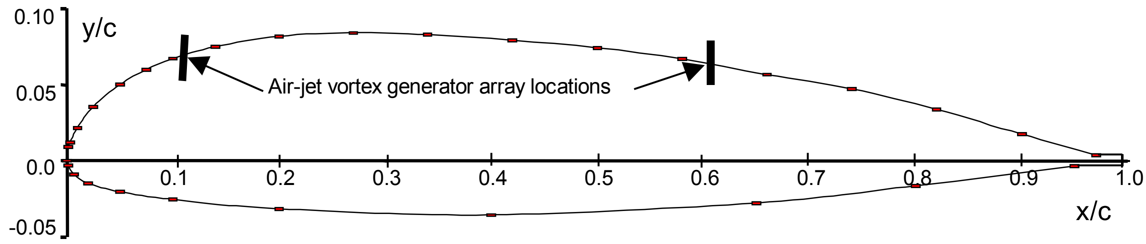

(a)

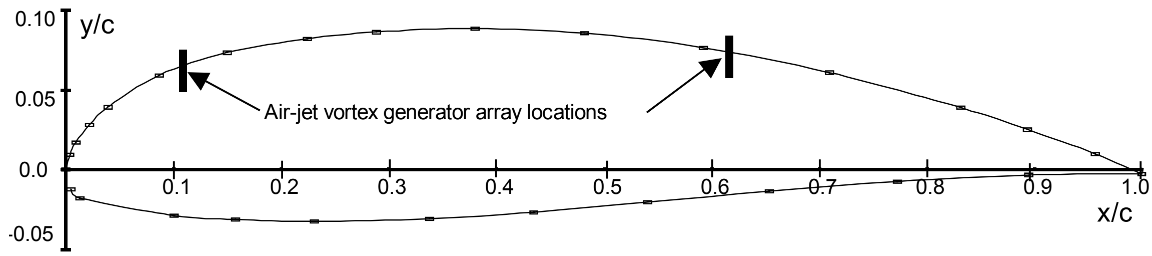

(b)

Figure 1: Chordwise profile of the (a) RAE 9645 and (b) NACA 23012C aerofoil sections indicating air-jet vortex generator locations at 12% and 62% chord

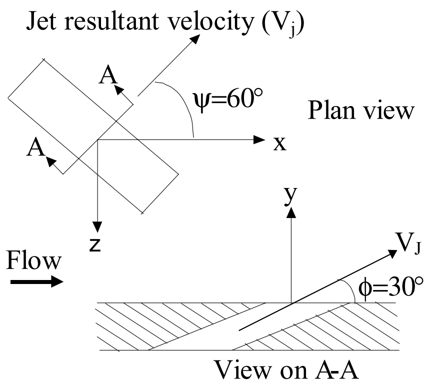

(a)

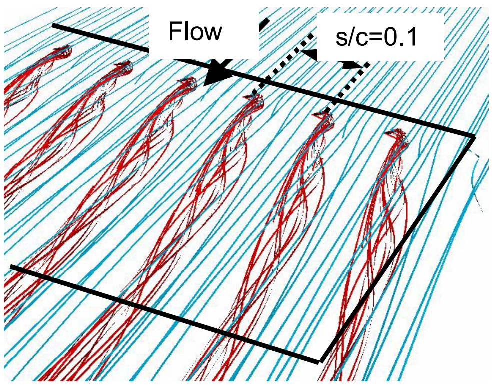

(b)

Figure 2: AJVG (a) geometrical configuration and (b) spacing and installation into aerofoil upper surface

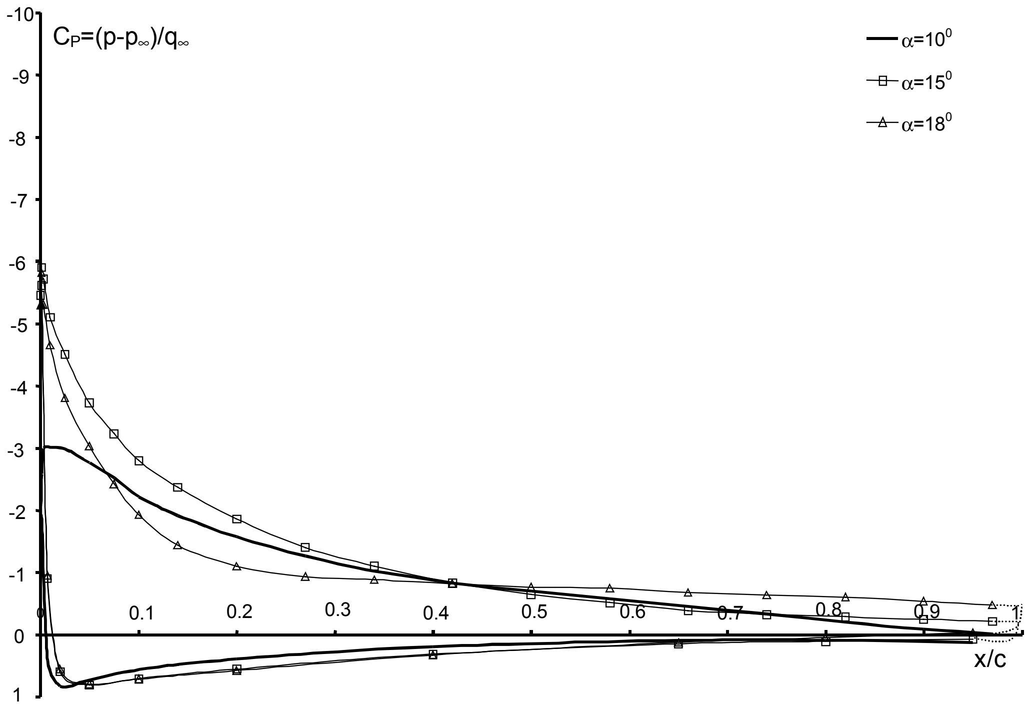

Figure 3: Sensitivity of chordwise surface pressure distributions to incidence close to stall, at centre span, with C_μ=0, for RAE 9645 aerofoil at Re_c=1.5x10^6 and M_∞=0.13

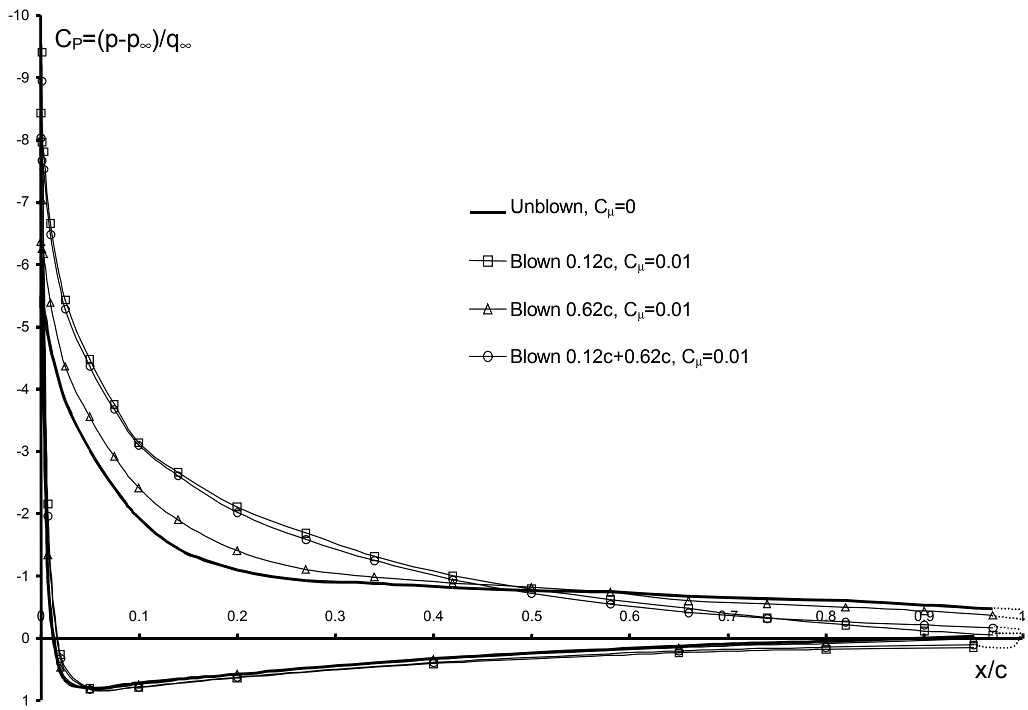

Figure 4: Sensitivity of chordwise surface pressure distributions to flow control with AJVGs for RAE 9645 aerofoil at α=18^0, Re_c=1.5x10^6 and M_∞=0.13

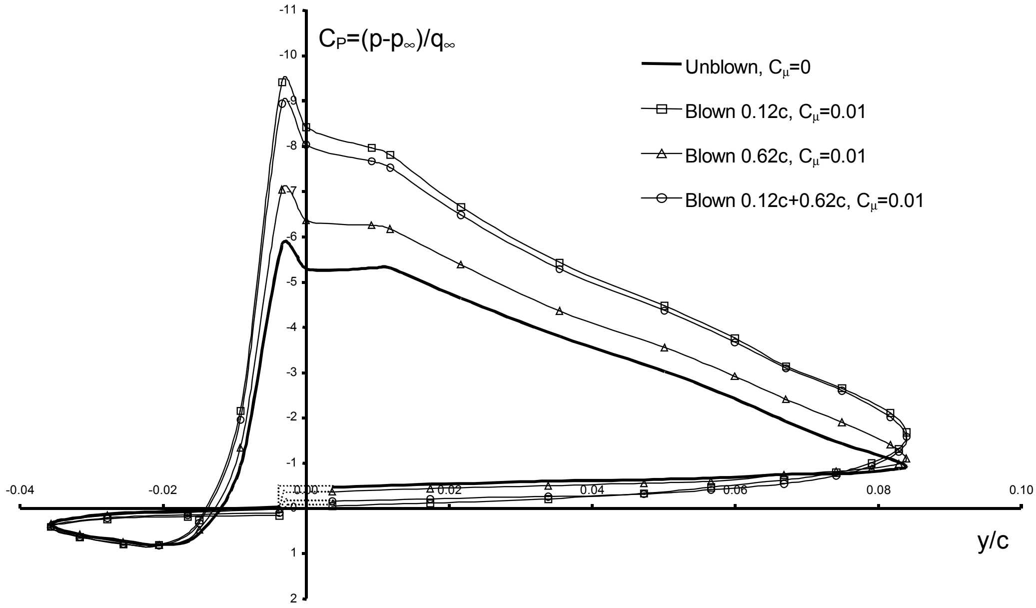

Figure 5: Sensitivity of leading edge suction to flow control with AJVGs for RAE 9645 aerofoil at $\alpha=18^0$, $Re_c=1.5\times10^6$ and $M_\infty=0.13$

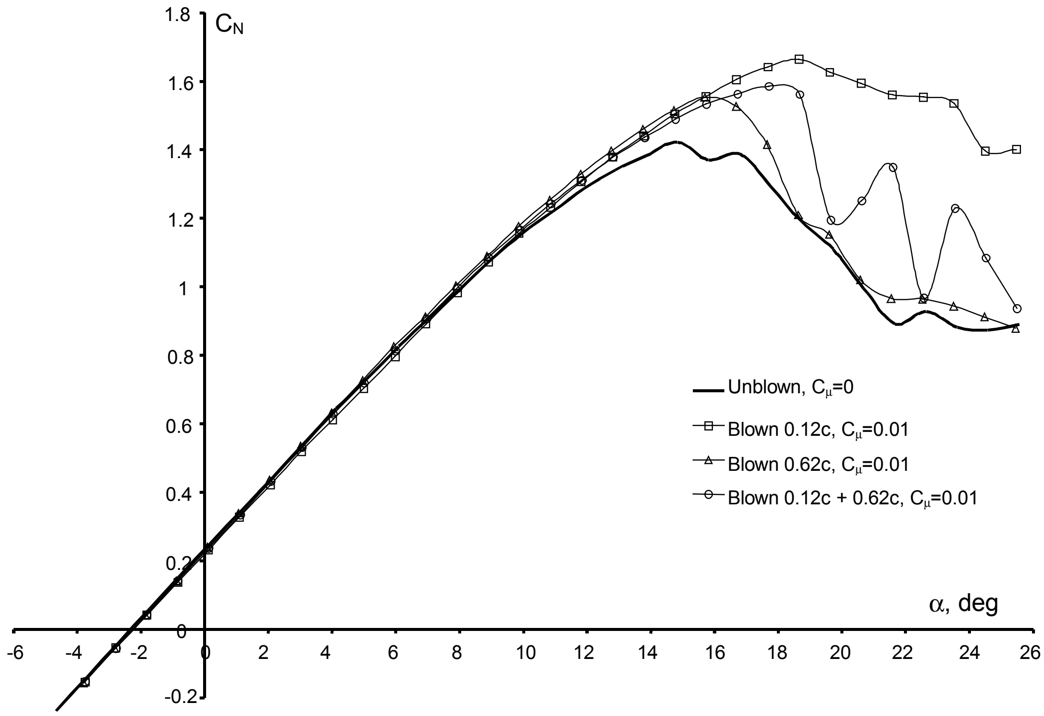

(a)

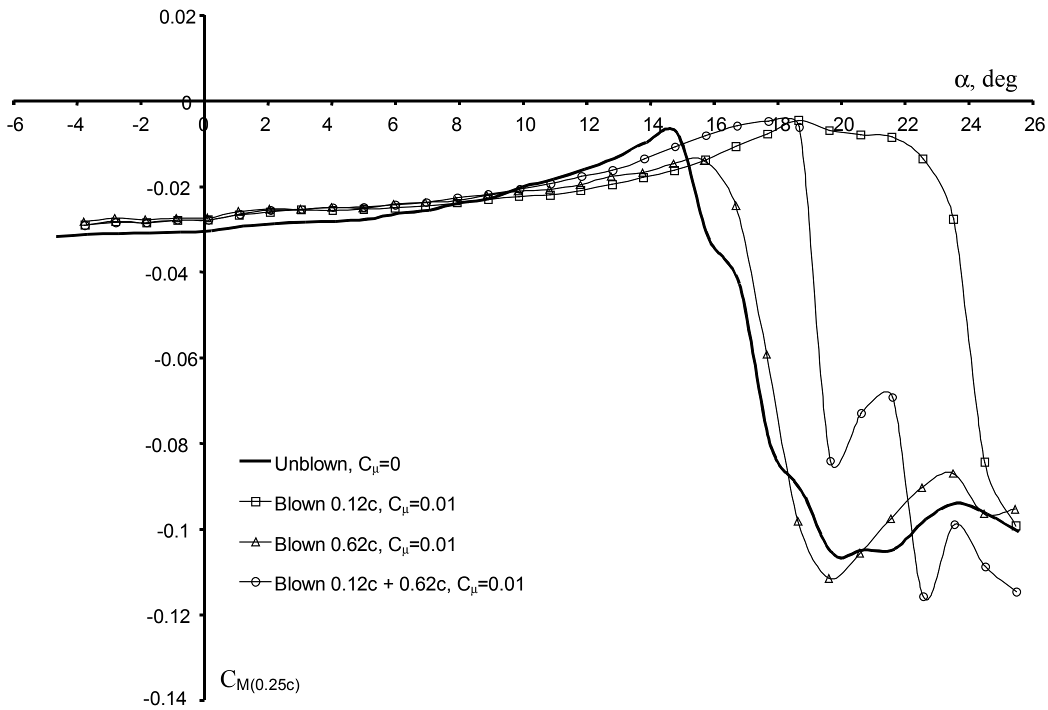

(b)

Figure 6: (a) Normal force coefficient and (b) quarter chord pitching moment coefficient variation with angle of attack for RAE 9645 aerofoil with AJVGs at Re_c=1.5x10^6 and M_∞=0.13

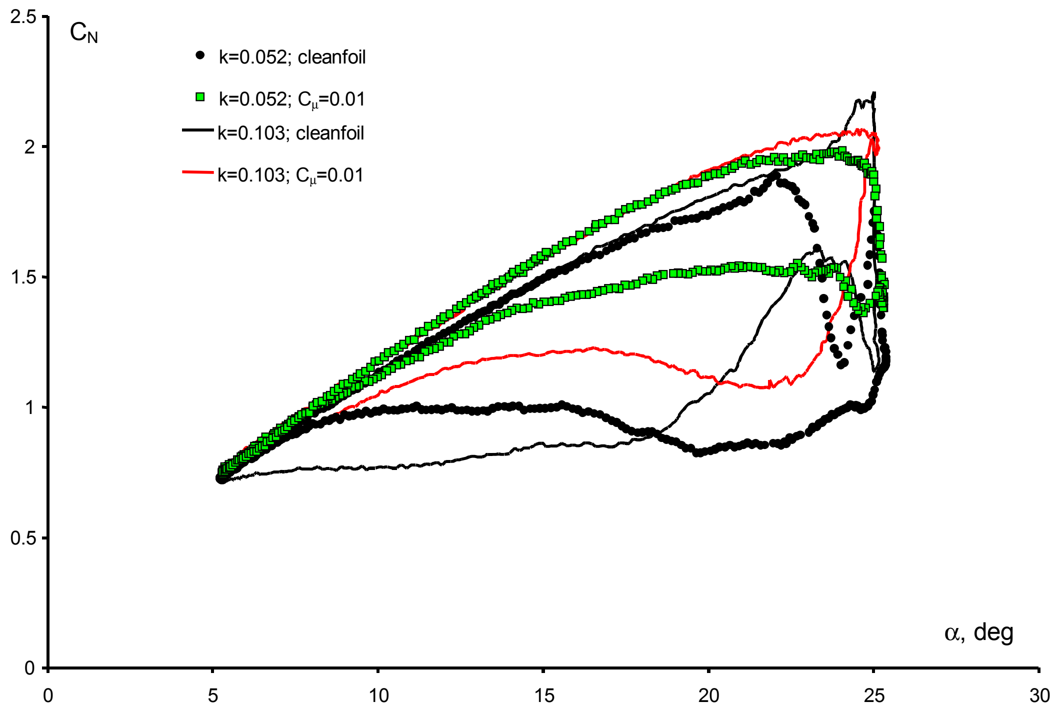

(a)

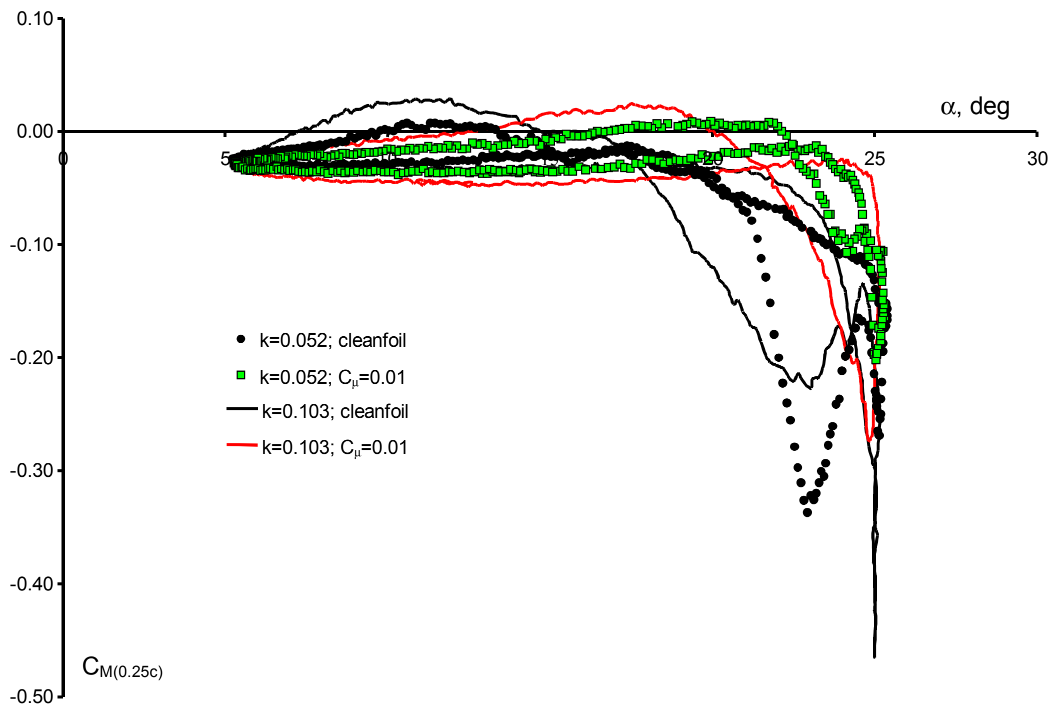

(b)

Figure 7: (a) Normal force and (b) quarter chord pitching moment coefficient, variation with angle of attack, for RAE 9645 oscillating aerofoil, at $Re_c=1.5\times10^6$, M=0.13, $\alpha=(15^0 + 10^0\sin\omega t)$, k=0.052 and 0.103

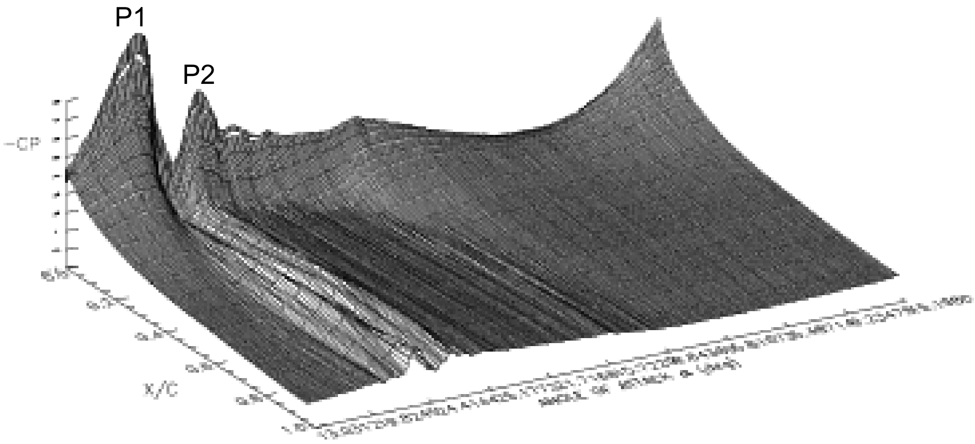

(a)

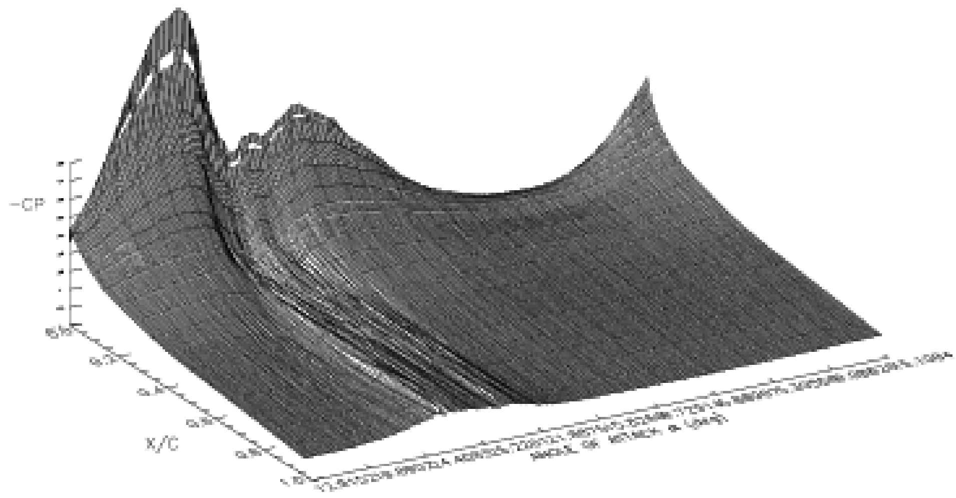

(b)

Figure 8: Instantaneous chordwise pressure distribution (a) cleanfoil and (b) front array AJVG blowing, C_μ=0.01 for RAE 9645 oscillating aerofoil, at Re_c=1.5x10^6, M=0.13, α=(15^0 + 10^0sinωt), k=0.052

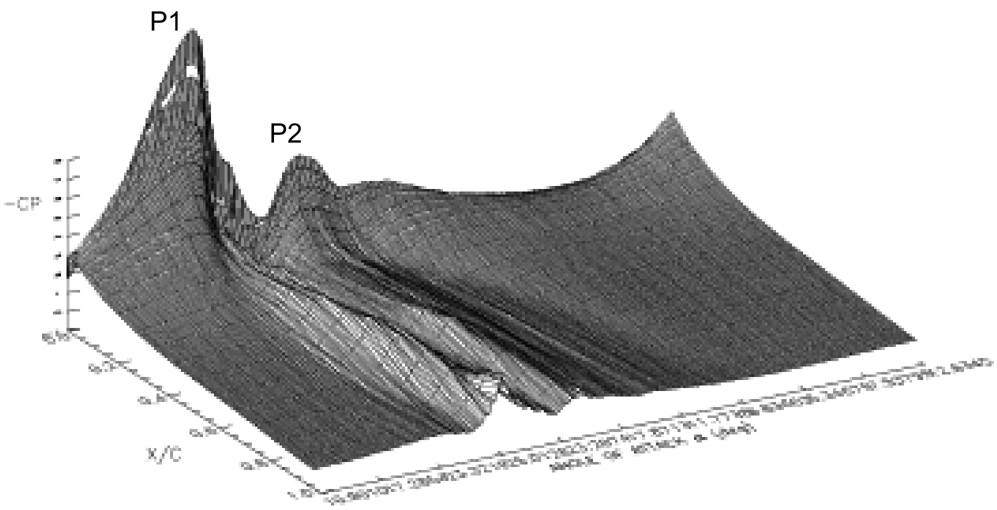

(a)

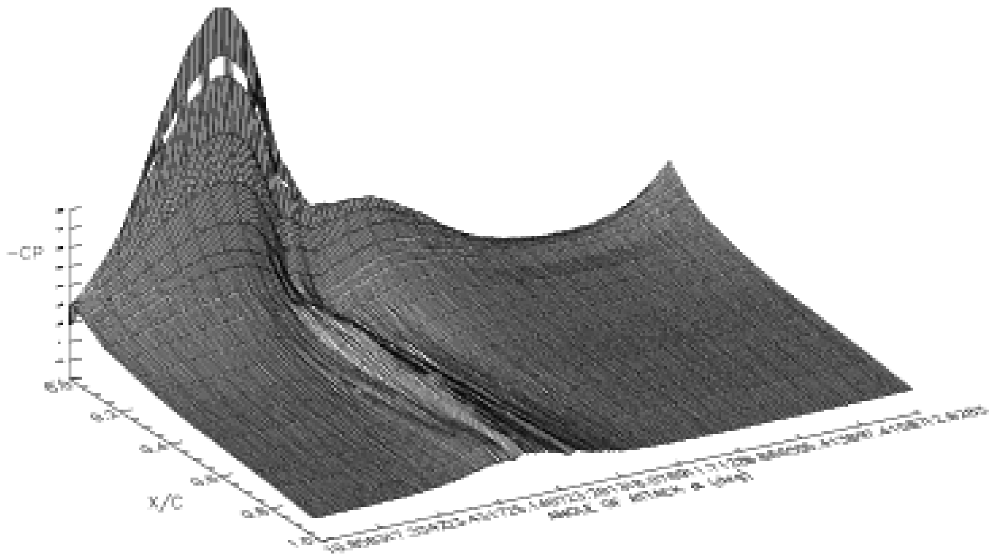

(b)

Figure 9: Instantaneous chordwise pressure distribution (a) cleanfoil and (b) front array AJVG blowing, C_{μ}=0.01 for RAE 9645 oscillating aerofoil, at Re_c=1.5x10^6, M=0.13, α=(15^0 + 10^{0}sinωt), k=0.103

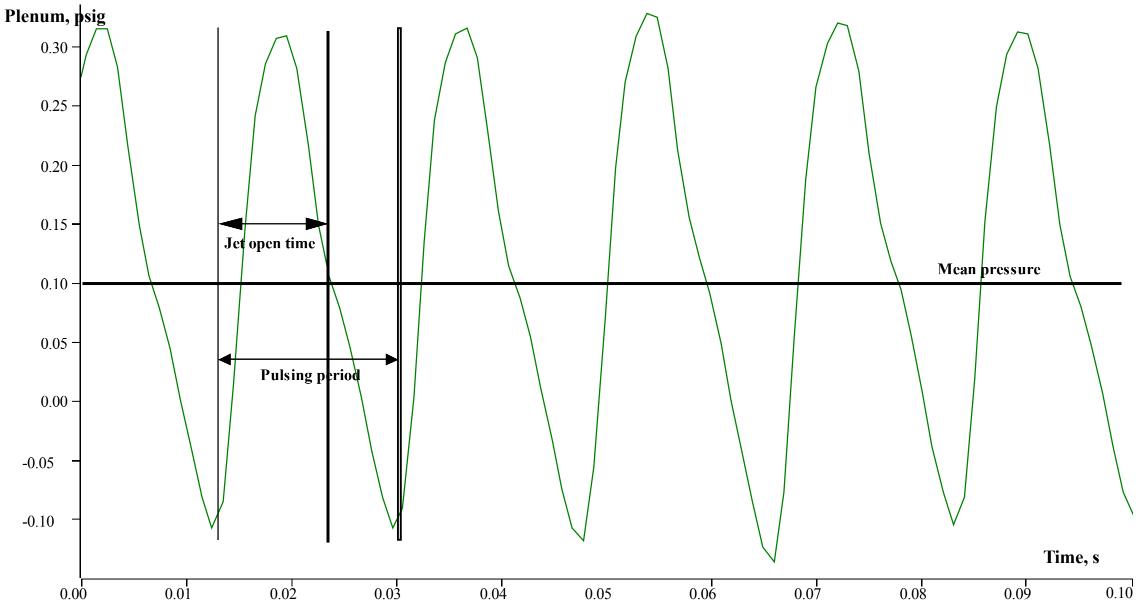

Figure 10: Example of pulse signal in the aerofoil plenum chamber at a mean and unsteady levels of 0.1psig and 0.078psig at F^{+}=0.7 and DC=0.65

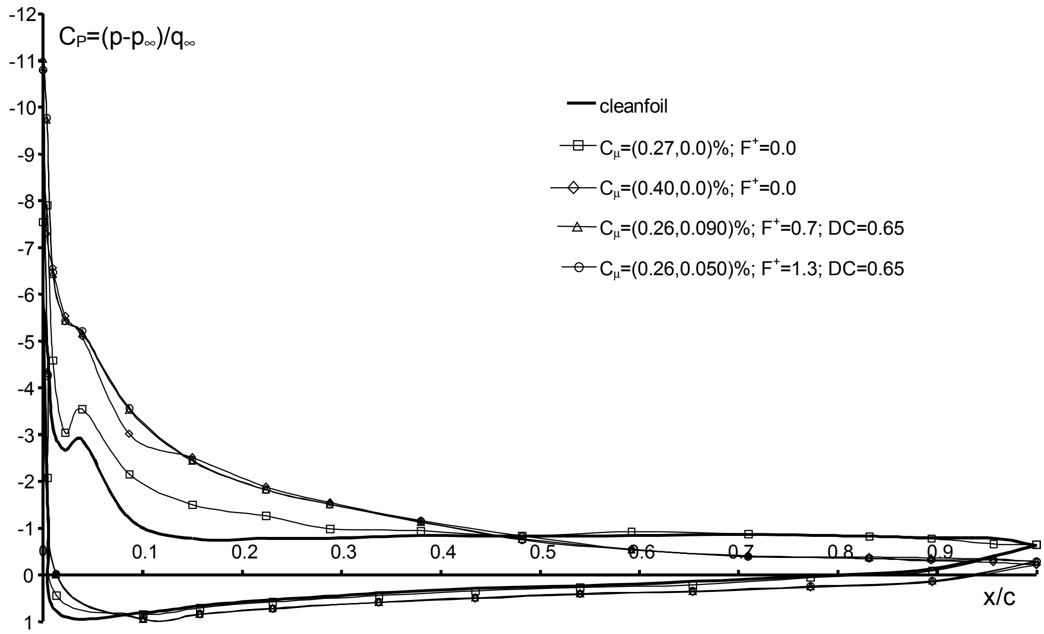

Figure 11: Sensitivity of chordwise surface pressure distribution to flow control with AJVGs for NACA 23012C aerofoil at $\alpha=20^0$, $Re_c=1.1\text{x}10^6$ and M_∞=0.12

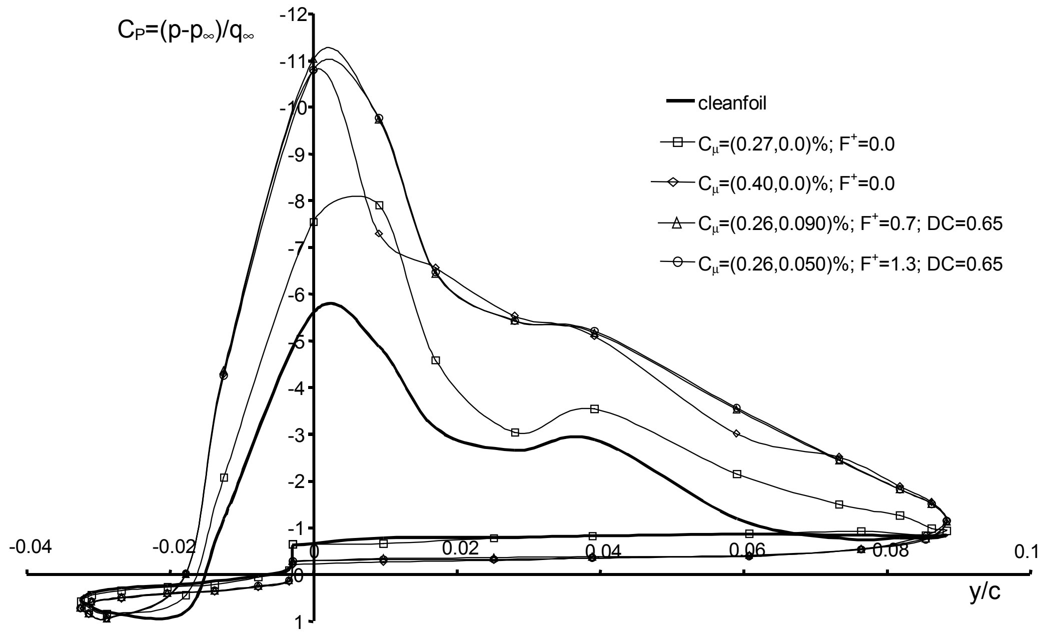

Figure 12: Sensitivity of leading-edge suction to flow control with AJVGs for NACA 23012C aerofoil at $\alpha=20^0$, $Re_c=1.1x10^6$ and $M_\infty=0.12$

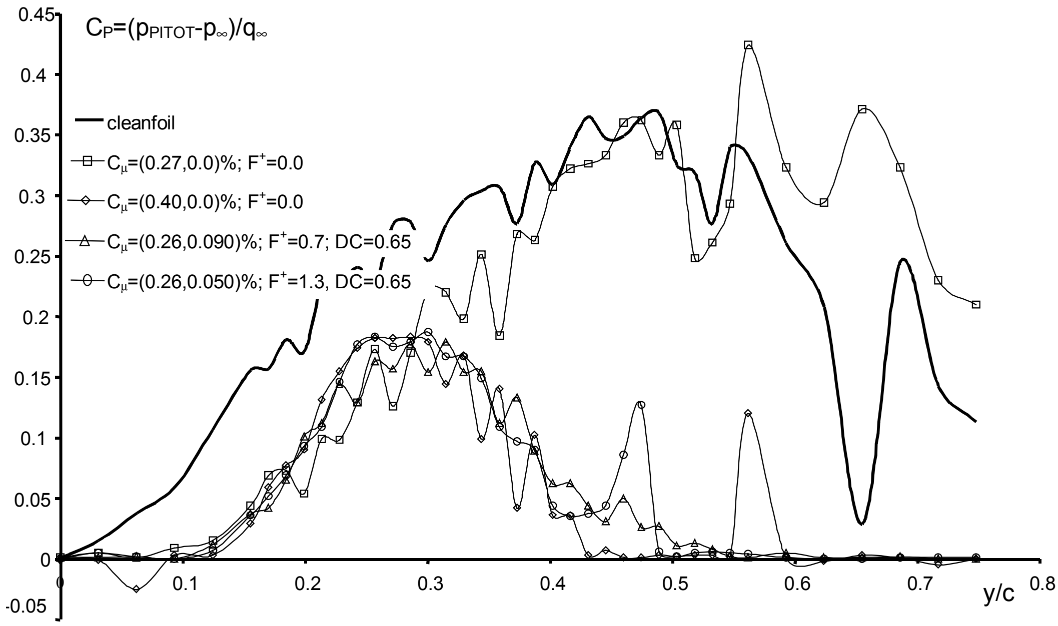

Figure 13: Wake profiles, measured one chord length downstream of the model trailing edge, for NACA 23012C aerofoil at $\alpha=20^0$, $Re_c=1.1x10^6$ and $M_\infty=0.12$